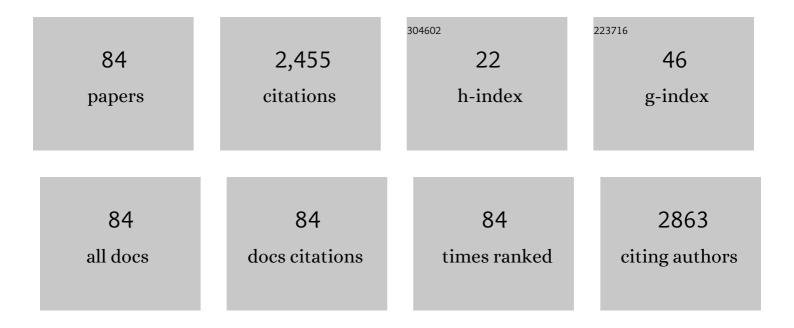
Chun-Hway Hsueh

List of Publications by Year in descending order

Source: https://exaly.com/author-pdf/5495814/publications.pdf Version: 2024-02-01



#	Article	IF	CITATIONS
1	Effects of La addition on the microstructure and mechanical properties of CoCrNi medium entropy alloy. Journal of Alloys and Compounds, 2022, 894, 162401.	2.8	18
2	Effects of yttrium addition on microstructures and mechanical properties of CoCrNi medium entropy alloy. Intermetallics, 2022, 140, 107405.	1.8	23
3	Subwavelength VO ₂ Nanoparticle Films for Smart Window Applications. ACS Applied Nano Materials, 2022, 5, 2923-2934.	2.4	10
4	Au-Based Thin-Film Metallic Glasses for Propagating Surface Plasmon Resonance-Based Sensor Applications. ACS Omega, 2022, 7, 18780-18785.	1.6	5
5	Wafer-scale SERS metallic nanotube arrays with highly ordered periodicity. Sensors and Actuators B: Chemical, 2021, 329, 129132.	4.0	16
6	Fatigue studies of CoCrFeMnNi high entropy alloy films using nanoindentation dynamic mechanical analyses. Surface and Coatings Technology, 2021, 410, 126927.	2.2	10
7	Kinetin Detection Enhancement Based on Photonic Nanojets and Surface-Enhanced Raman Scattering. IEEE Journal of Selected Topics in Quantum Electronics, 2021, 27, 1-8.	1.9	1
8	Nanotwinned CoCrFeMnNi high entropy alloy films for flexible electronic device applications. Vacuum, 2021, 189, 110249.	1.6	9
9	Structural and Optical Properties of Textured Silicon Substrates by Three-Step Chemical Etching. Langmuir, 2021, 37, 9622-9629.	1.6	4
10	Microstructures and mechanical properties of (CoCrFeMnNi)100-Mo high entropy alloy films. Intermetallics, 2021, 135, 107236.	1.8	13
11	Effects of cerium addition on microstructures and mechanical properties of CoCrNi medium entropy alloy films. Surface and Coatings Technology, 2021, 424, 127645.	2.2	10
12	Fabrication of periodic Ag tetrahedral nanopyramids via H2O2-assisted nanosphere lithography for plasmonic applications. Colloids and Surfaces A: Physicochemical and Engineering Aspects, 2021, 628, 127278.	2.3	4
13	Imprintable Au-Based Thin-Film Metallic Glasses with Different Crystallinities for Surface-Enhanced Raman Scattering. Journal of Physical Chemistry C, 2021, 125, 23983-23990.	1.5	4
14	Effects of Nb Addition on Microstructures and Mechanical Properties of Nbx-CoCrFeMnNi High Entropy Alloy Films. Coatings, 2021, 11, 1539.	1.2	12
15	Effects of Ag particle geometry on photocatalytic performance of Ag/TiO2/reduced graphene oxide ternary systems. Materials Chemistry and Physics, 2020, 240, 122216.	2.0	16
16	Microstructures and mechanical properties of CoCrFeMnNiV high entropy alloy films. Journal of Alloys and Compounds, 2020, 820, 153388.	2.8	52
17	Wettability, electron work function and corrosion behavior of CoCrFeMnNi high entropy alloy films. Surface and Coatings Technology, 2020, 400, 126222.	2.2	27
18	High hardness and fatigue resistance of CoCrFeMnNi high entropy alloy films with ultrahigh-density nanotwins. International Journal of Plasticity, 2020, 131, 102726.	4.1	80

#	Article	IF	CITATIONS
19	Modifications of microstructures and mechanical properties of CoCrFeMnNi high entropy alloy films by adding Ti element. Surface and Coatings Technology, 2020, 399, 126149.	2.2	19
20	Growth, microstructure and mechanical properties of CoCrFeMnNi high entropy alloy films. Vacuum, 2020, 179, 109553.	1.6	27
21	Martensitic transformation and mechanical behavior of a medium-entropy alloy. Materials Science & Engineering A: Structural Materials: Properties, Microstructure and Processing, 2020, 786, 139371.	2.6	18
22	Effects of Al Addition on Microstructures and Mechanical Properties of CoCrFeMnNiAlx High Entropy Alloy Films. Entropy, 2020, 22, 2.	1.1	35
23	Photocurrent Enhancements of TiO ₂ -Based Nanocomposites with Gold Nanostructures/Reduced Graphene Oxide on Nanobranched Substrate. Journal of Physical Chemistry C, 2019, 123, 21103-21113.	1.5	33
24	Fabrication of WO3 photoanode decorated with Au nanoplates and its enhanced photoelectrochemical properties. Electrochimica Acta, 2019, 321, 134674.	2.6	19
25	Hardness and strength enhancements of CoCrFeMnNi high-entropy alloy with Nd doping. Materials Science & Engineering A: Structural Materials: Properties, Microstructure and Processing, 2019, 764, 138192.	2.6	56
26	High quality thermochromic VO2 films prepared by magnetron sputtering using V2O5 target with in situ annealing. Applied Surface Science, 2019, 495, 143436.	3.1	44
27	Thermochromic vanadium dioxide film on textured silica substrate for smart window with enhanced visible transmittance and tunable infrared radiation. Infrared Physics and Technology, 2019, 102, 103019.	1.3	10
28	Construction of Schottky junction solar cell using silicon nanowires and multi-layered graphene. Superlattices and Microstructures, 2019, 126, 42-48.	1.4	11
29	Combined metal-assisted chemical etching and anisotropic wet etching for anti-reflection inverted pyramidal cavities on dendrite-like textured substrates. Results in Physics, 2019, 12, 244-249.	2.0	10
30	Surface plasmons excited by multiple layer grating. Optics Express, 2019, 27, 1660.	1.7	2
31	Micromechanics Modeling of Creep Fracture of High-Temperature Ceramics. , 2019, , 1035-1091.		Ο
32	Molecular Sensing and Color Manipulation Based on Dimension-Controlled Plasmon-Enhanced Silicon Nanotube SERS Substrates. Journal of Physical Chemistry C, 2018, 122, 8510-8516.	1.5	3
33	Nanoscaled superelastic behavior of shape memory alloy/metallic glass multilayered films. Composites Part B: Engineering, 2018, 142, 193-199.	5.9	20
34	Surface Plasmon Excited on Imprintable Thin-Film Metallic Glasses for Surface-Enhanced Raman Scattering Applications. ACS Applied Nano Materials, 2018, 1, 908-914.	2.4	11
35	High performance and reusable SERS substrates using Ag/ZnO heterostructure on periodic silicon nanotube substrate. Applied Surface Science, 2018, 439, 852-858.	3.1	31
36	TiNiCuAg shape memory alloy films for biomedical applications. Journal of Alloys and Compounds, 2018, 738, 336-344.	2.8	19

#	Article	IF	CITATIONS
37	Periodic ZnO-Elevated Gold Dimer Nanostructures for Surface-Enhanced Raman Scattering Applications. Journal of Physical Chemistry C, 2018, 122, 27016-27023.	1.5	5
38	Design of diffusion barrier and buffer layers for β-Zn4Sb3 mid-temperature thermoelectric modules. Journal of Alloys and Compounds, 2018, 762, 631-636.	2.8	7
39	Micromechanics Modeling of Creep Fracture of High-Temperature Ceramics. , 2018, , 1-58.		Ο
40	Improvement of photocatalytic activities of Ag/P25 hybrid systems by controlled morphology of Ag nanoprisms. Materials Chemistry and Physics, 2017, 192, 78-85.	2.0	14
41	Microstructure and mechanical properties of Zr-Ti-Cu-Nd metallic glass composites. Journal of Alloys and Compounds, 2017, 702, 318-326.	2.8	15
42	Suspended graphene with periodic dimer nanostructure on Si cavities for surface-enhanced Raman scattering applications. Applied Physics Letters, 2017, 110, 171111.	1.5	8
43	Viscous flow and viscosity measurement of low-temperature imprintable AuCuSi thin film metallic glasses investigated by nanoindentation creep. Materials and Design, 2017, 123, 112-119.	3.3	12
44	Far-field and near-field monitoring of hybridized optical modes from Au nanoprisms suspended on a graphene/Si nanopillar array. Nanoscale, 2017, 9, 16950-16959.	2.8	10
45	Mechanical properties and microstructure of Zr-Ti-Ni thin film metallic glasses modified with minor SF6. Composites Part B: Engineering, 2017, 129, 243-250.	5.9	10
46	Gold-rich ligament nanostructure by dealloying Au-based metallic glass ribbon for surface-enhanced Raman scattering. Scientific Reports, 2017, 7, 7485.	1.6	14
47	Free-standing gold elliptical nanoantenna with tunable wavelength in near-infrared region for enhanced Raman spectroscopy. Applied Physics A: Materials Science and Processing, 2016, 122, 1.	1.1	7
48	Effects of the rotation angle on surface plasmon coupling of nanoprisms. Nanoscale, 2016, 8, 3660-3670.	2.8	16
49	3D Nanostructures of Silver Nanoparticle-Decorated Suspended Graphene for SERS Detection. Journal of Physical Chemistry C, 2016, 120, 3448-3457.	1.5	18
50	Electroplastic forming in a Fe-based metallic glass ribbon. Journal of Alloys and Compounds, 2016, 658, 795-799.	2.8	13
51	Zr–Ti–Ni thin film metallic glass as a diffusion barrier between copper and silicon. Journal of Materials Science, 2015, 50, 2085-2092.	1.7	30
52	Optical Control of Fluorescence through Plasmonic Eigenmode Extinction. Scientific Reports, 2015, 5, 9911.	1.6	5
53	Anti-reflection textured structures by wet etching and island lithography for surface-enhanced Raman spectroscopy. Applied Surface Science, 2015, 357, 615-621.	3.1	20
54	Finite Element Analysis and Design of Thermal–Mechanical Stresses in Multilayer Ceramic Capacitors. International Journal of Applied Ceramic Technology, 2015, 12, 451-460.	1.1	17

#	Article	IF	CITATIONS
55	Effects of corner radius on periodic nanoantenna for surface-enhanced Raman spectroscopy. Journal of Optics (United Kingdom), 2015, 17, 125002.	1.0	13
56	Optimized Sensitivity and Electric Field Enhancement by Controlling Localized Surface Plasmon Resonances for Bowtie Nanoring Nanoantenna Arrays. Plasmonics, 2015, 10, 553-561.	1.8	22
57	Superelasticity of TiNi-based shape memory alloys at micro/nanoscale. Journal of Materials Research, 2014, 29, 2717-2726.	1.2	7
58	Rapid thermoplastic formation of Fe-based metallic glass foil achieved by electropulsing. Materials Letters, 2014, 136, 353-355.	1.3	10
59	Advanced characterization of mechanical properties of multilayer ceramic capacitors. Journal of Materials Science: Materials in Electronics, 2014, 25, 627-634.	1.1	12
60	Control of Stress Concentration in Surfaceâ€Mounted Multilayer Ceramic Capacitor Subjected to Bending. Journal of the American Ceramic Society, 2014, 97, 1170-1176.	1.9	7
61	Micromechanics modeling of creep fracture of zirconium diboride–silicon carbide composites at 1400–1700°C. Journal of the European Ceramic Society, 2014, 34, 4145-4155.	2.8	22
62	Thin film metallic glass as an underlayer for tin whisker mitigation: A room-temperature evaluation. Thin Solid Films, 2014, 561, 93-97.	0.8	14
63	Effects of annealing on mechanical behavior of Zr–Ti–Ni thin film metallic glasses. Materials Science & Engineering A: Structural Materials: Properties, Microstructure and Processing, 2014, 608, 258-264.	2.6	37
64	A micromechanics study of competing mechanisms for creep fracture of zirconium diboride polycrystals. Journal of the European Ceramic Society, 2013, 33, 1625-1637.	2.8	11
65	Rapid relaxation and embrittlement of Zr-based bulk metallic glasses by electropulsing. Intermetallics, 2013, 34, 43-48.	1.8	10
66	Giant Electric Field Enhancement and Localized Surface Plasmon Resonance by Optimizing Contour Bowtie Nanoantennas. Journal of Physical Chemistry C, 2013, 117, 25004-25011.	1.5	45
67	Plasticity enhancement of Zr-based bulk metallic glasses by direct current electropulsing. Journal of Alloys and Compounds, 2012, 525, 68-72.	2.8	19
68	Effects of grain boundary heterogeneities on creep fracture studied by rate-dependent cohesive model. Engineering Fracture Mechanics, 2012, 93, 48-64.	2.0	15
69	Novel method to measure the shear strength of exfoliated montmorillonite/polymer nanocomposite films. Polymer International, 2012, 61, 174-179.	1.6	3
70	High Tunability of the Surface-Enhanced Raman Scattering Response with a Metalâ^'Multiferroic Composite. Nano Letters, 2011, 11, 1265-1269.	4.5	22
71	Resonance modes, cavity field enhancements, and long-range collective photonic effects in periodic bowtie nanostructures. Optics Express, 2011, 19, 19660.	1.7	16
72	Measurements of residual stresses in Al film/silicon nitride substrate microcantilever beam systems. Journal of Materials Research, 2011, 26, 1279-1284.	1.2	5

#	Article	IF	CITATIONS
73	Free-Standing Optical Gold Bowtie Nanoantenna with Variable Gap Size for Enhanced Raman Spectroscopy. Nano Letters, 2010, 10, 4952-4955.	4.5	480
74	Controlled normal/shear loading and shear fracture in bulk metallic glasses. Intermetallics, 2009, 17, 802-810.	1.8	8
75	Shear fracture of bulk metallic glasses with controlled applied normal stresses. Scripta Materialia, 2008, 59, 111-114.	2.6	18
76	Analyses of mode I edge delamination by thermal stresses in multilayer systems. Composites Part B: Engineering, 2006, 37, 1-9.	5.9	27
77	Master curves for Hertzian indentation on coating/substrate systems. Journal of Materials Research, 2004, 19, 94-100.	1.2	40
78	Combined empirical–analytical method for determining contact radius and indenter displacement during Hertzian indentation on coating/substrate systems. Journal of Materials Research, 2004, 19, 2774-2781.	1.2	30
79	Effects of viscous flow on residual stresses in film/substrate systems. Journal of Applied Physics, 2002, 91, 2760-2765.	1.1	23
80	Modeling of elastic deformation of multilayers due to residual stresses and external bending. Journal of Applied Physics, 2002, 91, 9652.	1.1	283
81	Apparent coefficient of thermal expansion and residual stresses in multilayer capacitors. Composites Part A: Applied Science and Manufacturing, 2002, 33, 1115-1121.	3.8	17
82	Thermal stresses in elastic multilayer systems. Thin Solid Films, 2002, 418, 182-188.	0.8	234
83	A damage model of creep crack growth in polycrystals. Acta Metallurgica, 1983, 31, 1675-1687.	2.1	55
84	Overview 14 Creep fracture in ceramic polycrystals—II. effects of inhomogeneity on creep rupture. Acta Metallurgica, 1981, 29, 1907-1917.	2.1	47